Title

Warm-season precipitation drivers in northeastern Argentina: diurnal cycle of the atmospheric moisture balance and land-atmosphere coupling

Short Title

Warm-season precipitation drivers in northeastern Argentina

Authors

Julián Alberto Giles*(1,3,4), Romina Carla Ruscica(1,3,4), Claudio Guillermo Menéndez(2,3,4)

(1) Universidad de Buenos Aires, Facultad de Ciencias Exactas y Naturales. Buenos Aires, Argentina.

(2) Universidad de Buenos Aires, Facultad de Ciencias Exactas y Naturales, Departamento de Ciencias de la Atmósfera y los Océanos. Buenos Aires, Argentina.

(3) CONICET – Universidad de Buenos Aires. Centro de Investigaciones del Mar y la Atmósfera (CIMA). Buenos Aires, Argentina.

(4) CNRS – IRD – CONICET – UBA. Instituto Franco-Argentino para el Estudio del Clima y sus Impactos (UMI 3351 IFAECI). Buenos Aires, Argentina.

This article has been accepted for publication and undergone full peer review but has not been through the copyediting, typesetting, pagination and proofreading process which may lead to differences between this version and the Version of Record. Please cite this article as doi: 10.1002/joc.6724

*Corresponding author: julian.giles@cima.fcen.uba.ar - Intendente Güiraldes 2160 - Ciudad Universitaria - Pabellón II - 2do. piso (C1428EGA) Buenos Aires - Argentina. Tel: (54)(11) 5285-8467 - Fax: (54)(11) 4788-3572

Keywords

Diurnal cycle, Model experiments, Land atmosphere coupling, Precipitation, Atmospheric Water balance, South American low level jet

Funding Information

LEFE (CNRS, France), Grant number: AO2015-876370

PIP (CONICET, Argentina), Grant number: 112-201101-00932

PICT (ANPCyT, Argentina), Grant number: 2015-3097

Abstract

Southeastern South America is influenced by moisture transport from lower latitudes, sustains intense convective storms and is a land-atmosphere coupling hotspot, but the interconnection between these processes is still not well understood. We present the warm-season diurnal cycle climatology of the water balance components in the South American Low-Level Jet (SALLJ) exit region in northeastern Argentina during 1998-2012. Different precipitation-based types of events (clear-sky and rainy days) were explored together with processes tied to the land-atmosphere coupling at the daily scale. Our research was based on simulations with and without soil moisture-atmosphere coupling with the RCA4 regional climate model. A control simulation was compared with a sensitivity simulation where the soil moisture was prescribed with the daily climatological values from the control run. The ERA5 reanalysis and the satellite precipitation products TRMM-3B42 v7 and CMORPH v1.0 bias corrected were used for comparative purposes. From the diurnal water balance analysis we found that moisture flux convergence in the region is the main driver for nocturnal precipitation while local evapotranspiration feeds afternoon rain events. Rainy afternoons do not show differences between simulations, but rainy nights seem to be affected. Moreover, daily correlations between surface and boundary-layer variables showed that the local coupling is weaker during rainy days than during clear-sky days. Therefore, we suggest that changes in non-local drivers, such as the moisture flux through the SALLJ, are more relevant for rainy nights than the local coupling.

Introduction

The hydrological cycle in a region is built on advected moisture from remote sources and on local water recycling processes. Southeastern South America receives most of its moisture from the Atlantic Ocean, and from the tropical Amazon which is transported along the Andes by the South American Low-Level Jet (SALLJ) (Teitelbaum et al., 2008; Martinez and Dominguez, 2014). The SALLJ moisture transport maximizes during the warm season (Saulo et al., 2000; Berbery and Barros, 2002; Marengo et al., 2004; Vera et al., 2006) when its exit region is mainly located south of 25°S from northern Argentina to southern Brazil. The SALLJ exhibits variability in multiple scales from diurnal -with a nocturnal maximum- to multidecadal (Berbery and Collini, 2000; Marengo et al., 2004; Jones and Carvalho, 2018; Montini et al., 2019) and, unlike the low-level jet of the North American Southern Great Plains, occurs all year round.

Evapotranspiration also contributes from the surface to the atmospheric water cycle in terms of moisture recycling but also in terms of boundary layer instability that could lead to rainfall generation (e.g. Eltahir, 1998; Taylor et al., 2012; Tawfik et al., 2015). These processes intensify in summer when the atmospheric demand is the highest. In particular, the SALLJ exit region is located within the La Plata Basin, where continental moisture recycling highly contributes to local precipitation (van der Ent et al., 2010; Martinez and Dominguez, 2014; Zemp et al., 2014) and is also known as a hotspot of land-atmosphere coupling, where surface fluxes depend on soil moisture conditions. Some land-atmosphere interaction studies have been done at the interannual and intraseasonal time scale in this region (Ruscica et al., 2014, 2015, 2016; Spennemann et al., 2018; Menéndez et al., 2019); however, many land-atmosphere processes are still poorly understood, mainly at the diurnal scale and especially how they influence precipitation. In general, global and regional studies have found that the coupling seems to favor

afternoon precipitation preferably over strong soil moisture gradients (Taylor et al., 2011; Petrova et al., 2018), but its magnitude and the signal of the feedbacks can change depending on the background wind (Froidevaux et al., 2014; Ford et al., 2015; Holgate et al., 2019) and the moisture flux convergence (Petrova et al., 2018; Welty and Zeng, 2018). Moreover, the coupling can be strong in certain synoptic/mesoscale situations but weak or non-existent in the overall mean (Song et al., 2016; Welty and Zeng, 2018) and it can vary widely depending on the type of dataset analyzed (observation-derived products, models, reanalyses, etc.) (Taylor et al., 2012; Guillod et al., 2014) and the parameterizations used in models (Taylor et al., 2013; Ford et al., 2015).

A better understanding of the warm-season water cycle and related land-atmosphere processes at the diurnal scale in the SALLJ exit region is relevant in terms of hydrological–climatic impacts. The diurnal cycle of precipitation in this region is marked by frequent and intense nocturnal precipitation as a conjunction of convective systems and enhanced low-level convergence associated with the SALLJ (Nicolini and Saulo, 2006). However, regional climate models (RCMs) usually struggle to correctly simulate the diurnal cycle of precipitation by having more frequent afternoon precipitation, having mean peak precipitation in the afternoon hours and/or overestimating the frequency of light rainfall and underestimating that of intermediate or intense rain events (da Rocha et al., 2009; Reboita et al., 2016; Giles et al., 2019). Consequently, these issues could affect the distribution of extreme events or result in a correct representation of total mean precipitation but due to cancelation of errors (Carril et al., 2012). The errors in precipitation simulation are at least partly related to land-surface processes (Solman et al., 2013).

The aim of this paper is to disentangle the soil moisture-atmosphere coupling over a specific region under certain atmospheric events. We present a daily and diurnal climatological characterization of the atmospheric conditions for clear-sky, rainy-afternoon and rainy-night days to explore if and how the correspondent moisture balance and land-atmosphere coupling are related during the warm season in the SALLJ exit region. In particular, we describe the strengths and limitations of an RCM to simulate precipitation and its diurnal cycle, as well as the coupling between various boundary layer variables, in different rainfall regimes. Data from the RCA4 RCM and the novel ERA5 global reanalysis were employed for the characterization and an RCA4 sensitivity experiment was done for exploring the coupling. The two satellite-based precipitation products TRMM-3B42 TMPA v7 and CMORPH v1.0 were used as reference.

Methodology

Data and region description

We analyze 15 years (1998-2012) of hourly data from the recent ERA5 reanalysis (C3S 2017; Hersbach et al. 2019) and from a simulation with the SMHI Rossby Centre regional climate model, RCA4 (Kupiainen et al., 2014), driven by ERA-Interim over the whole South American continent. ERA5 has a finer spatial and temporal resolution and a better global balance of precipitation and evaporation than ERA-Interim, among other improvements (C3S, 2017). The version of RCA4 considered in this study is currently used within CORDEX (http://www.cordex.org) and has been used over Southeastern South America in previous studies (Spennemann et al., 2018; Falco et al., 2019; Giles et al., 2019; Menéndez et al., 2019; Zaninelli et al., 2019), to which the reader can refer for more information about the model's

configuration and performance. The spatial resolution is 25 km and 50 km for ERA5 and RCA4 respectively. We also employed two quasi-global multi-satellite precipitation analysis datasets: TRMM-3B42 TMPA v7 (Huffman et al., 2007, 2009; Tropical Rainfall Measuring Mission, 2011) and CMORPH v1.0 bias corrected (Joyce et al., 2004; Xie et al., 2017; Climate Prediction Center, 2018). Both precipitation products (from now on TRMM-3B42 and CMORPH, respectively) come at 3 hourly temporal resolution and about 25 km spatial resolution.

In addition to the control RCA4-run (hereafter CTL) we performed a second run where the land-surface is uncoupled from the atmosphere (hereafter UNC) by prescribing the soil moisture of each time step using the corresponding CTL soil moisture climatology of the given day. The CTL and UNC simulations have identical soil moisture climatologies, but in UNC soil moisture does not respond to either precipitation or evapotranspiration. Hence, the UNC run eliminates interannual and intra-diurnal variations of soil moisture, though it retains its mean annual cycle (inter-daily variability). Then, comparing CTL and UNC, it is possible to isolate the influence that soil moisture variability has on the atmosphere in order to study causality (e.g. Ruscica et al., 2015). This pair of simulations was also analyzed in Menéndez et al. (2019) in the context of surface air temperature variability and the reader can refer to that study for more information regarding the experiment set-up and the characteristics of the soil-atmosphere coupling.

The analyses described below were based on areal means in the SALLJ exit region in northeastern Argentina, hereafter referred to as JEXIT, defined between 25-30°S and 62-58°W (Figure 1, red box). The study is focused on the warm season, extending from October to March, and we worked using local solar time (LST = UTC-4).

Event classification

We classified different precipitation events following a strategy similar to Zhang and Klein (2010) and Tao et al. (2019). From a total of 2732 days (15 semesters) we selected days based on domain-averaged precipitation (P) and cloud cover according to the following criteria:

- Clear-sky days: P = 0 during all hours. Total cloud cover < 15% and low cloud cover < 5% from 8 to 16 LST.
- Rainy-afternoon days: the maximum P rate is greater than 1 mm/day, located between 12 and 21 LST and greater than 1.5 times the precipitation rates outside the 12-21 LST range. Also, the maximum P rate is less than 1 mm/day between 0 and 10 LST.
- Rainy-night days: the maximum P rate is greater than 1 mm/day and located between 0 and 6 LST.

This classification selects a sub-sample of the total amount of days in the period since there are situations where none of the above criteria are met: for example days with no precipitation but high cloud cover, or days with heavy precipitation both during daytime and nighttime. Clear-sky days were analyzed only for ERA5 and RCA4 since the criterion includes cloud cover in addition to P.

Analysis methods based on water and energy budgets

The hourly diurnal cycle composites of area-averaged P, evapotranspiration (E), vertically integrated moisture flux convergence (MFC, i.e. negative moisture flux divergence, MFD) and rate of change of atmospheric precipitable water (dPW) are calculated for rainy-afternoon and

rainy-night days for both RCA4 (CTL and UNC) and ERA5 datasets together with the composites of P for TRMM-3B42 and CMORPH. These variables are involved in the atmospheric water balance according to the equation (Rasmusson, 1968):

$$P - E = -dPW - MFD \quad (1)$$

That is, the deficit (excess) of atmospheric moisture from the difference between P and E must be compensated by water being extracted from (stored in) the atmosphere and/or by moisture being transported inside (outside) of the region via moisture convergence (MFD<0) or divergence (MFD>0).

Additionally, we calculate the mean daily amounts of water-balance components for each type of event for RCA4 (CTL and UNC) and ERA5. The daily values are computed from 9 LST of the previous day to 9 LST of the event day for rainy-night days, and from midnight to midnight for the other regimes, so that the precipitation event lands at the end of the 24 h period.

The energy budget equation links the net surface radiation (the sum of net longwave radiation, LWR, and net shortwave radiation, SWR) with the surface heat fluxes (sensible heat flux, SHF; latent heat flux, LHF), therefore, the daily variability of the balance may depend partially on the variability of the land state in coupling zones. To investigate the coupling between the soil moisture state (SM), the processes involved in the energy balance (SWR, LWR, SHF, LHF) and selected atmospheric variables (evaporative fraction, EF; planetary boundary layer height, PBLH; 2-meter temperature, T2m; 2-meter specific humidity, Q2m; moist static energy at 900 hPa, MSE) in JEXIT, the linear correlation coefficients between all possible pairs of daily anomalies of these variables were calculated for the CTL and UNC experiments and for the

different event types. Daily anomalies are calculated by removing the climatological monthly mean.

Results

Characteristics of selected days

Figure 1 shows ERA5's vertically integrated moisture flux and its convergence in the region surrounding JEXIT. The results for RCA4 are similar (not shown). We observe the climatological pattern (Figure 1 a) of intense moisture flux along the eastern slope of the Andes through Bolivia and Paraguay, which weakens in northern Argentina. This pattern changes radically during JEXIT clear-sky days (Figure 1 b), the intense pattern to the east of the Bolivian Andes disappears and a small stripe of high moisture flux and convergence is located in northwestern Argentina driven by an anticyclonic gyre centered in eastern Argentina. For rainy days (Figure 1 c,d) the moisture flux pattern intensifies compared to the climatology and points towards northwestern (northeastern) Argentina for rainy-afternoon (rainy-night) days. In rainy-afternoon days there is a moisture convergence maximum located just west and south of JEXIT, while during rainy-night days a wide belt of intense moisture convergence includes almost all of JEXIT.

Figure 2 shows the diurnal cycle of P, E, MFC and dPW for selected rainy days. ERA5 and RCA4-CTL agree on a narrow afternoon rainfall peak (Figure 2 a,c) and a wider and more intense rainfall event during nights (Figure 2 b,d). In particular for rainy afternoons, ERA5 shows that the conditions preceding the event include high values of E and positive dPW (over 12 mm/day), with little MFC (under 4 mm/day). The rainfall event then occurs with a maximum

around 16 LST and, right after, MFC comes close to zero and dPW becomes negative, i.e., there is a slight depletion of precipitable water. RCA4-CTL shows a similar behavior with positive low MFC and high E and dPW (although lower than ERA5, around 6 mm/day) before the maximum of precipitation which is around two hours ahead of that of ERA5. Therefore, rainy-afternoon events are mainly driven by local soil water supply. The percentage of afternoon events in ERA5 and RCA4-CTL is quite similar (around 6%) and slightly higher than those in TRMM-3B42 and CMORPH (around 5%). In addition, the intensity of the events in ERA5 and RCA4-CTL is also similar (around 3.5 mm/day) but considerably lower than the ones in the satellite products, suggesting a possible underestimation of peak precipitation.

In the case of rainy nights, ERA5 and RCA4-CTL also show similar results: high positive MFC (up to 12 mm/day in RCA-CTL and over that in ERA5) in the region with low dPW just before the precipitation maximum, which is located around 3 LST, and intense depletion of atmospheric water occur after the event. Rainy nights are consequently driven by MFC, that is, by external water supply. Differently to afternoon events, ERA5 has about three times more nighttime events (around 18%) than RCA4 (around 6%), with satellite products in between (11%), suggesting a possible overestimation (underestimation) of the frequency of rainy nights by ERA5 (RCA4). Similarly to afternoon events, the intensity in both ERA5 and RCA4-CTL rainy nights is comparable (around 20 mm/day) and about 30% lower than that detected by satellites.

From another perspective, Figure 3 shows the mean daily amounts of water-balance components for the different types of precipitation days. At first glance we note that RCA4 and ERA5 give qualitatively the same results, with some quantitative differences. Rainy-night days have P values notoriously higher than rainy-afternoon days while E is similar in both cases,

consequently P-E results positive in the former and negative in the latter. We observe that both regimes have positive MFC, however, it is remarkably important for rainy-night days (around 10 mm/day), where it is higher than E (around 4 mm/day). The dPW is different for both regimes, with positive values comparable to E for rainy-afternoon days, and negative values for rainy-night days. That means that on rainy-afternoon (rainy-night) days the atmosphere typically ends up gaining (losing) water, even though both regimes have precipitation.

From Figure 3 we support the analysis of Figure 2, where on rainy-afternoon days there is a stronger local forcing through E that accumulates moisture in the atmosphere and initiates the precipitation event, and a different situation builds up in rainy-night days where an important external forcing (MFC) drives an intense rainfall event that ends up reducing the available moisture in the atmosphere. In clear-sky days E is similar to that of days with precipitation, accompanied by MFD and positive dPW. However we observe a difference in behavior between datasets, while E is greater in clear-sky days than in rainy days in ERA5, RCA4 shows the opposite: lower E in clear-sky days and greater E in days with precipitation. Nonetheless, it should be noted that the moisture budget for the JEXIT region is not closed in ERA5 as evidenced by the non-negligible residuals from Equation 1 for all three regimes, which are the same order of magnitude as the differences in E.

Land-atmosphere coupling

To analyze the impacts of soil moisture on the variability of different variables, we compare the CTL and UNC experiments. The diurnal cycle composites (Figure 2 d) show that during rainy nights the precipitation intensity decreases in the coupled experiment (CTL), particularly at the

time of maximum rainfall and some hours before, but the frequency of events is higher in CTL. Lower precipitation intensity is consistent with less MFC in CTL during the hours previous to the nocturnal rain event, also seen in the daily mean values (Figure 3). On the other hand, rainy afternoons are not affected by the land-atmosphere coupling for the most part (Figure 2 c and Figure 3), suggesting that the stability of the free troposphere also plays a role.

The evapotranspiration regime in JEXIT is in general limited by SM (Sörensson and Menéndez, 2011; Menéndez et al., 2016), therefore SM variability can potentially impact other variables, particularly in events less influenced by moisture advection from other regions. For clear-sky days in the CTL experiment (Figure 4 a), a negative SM anomaly promotes more SHF and less Q2m (from reduced LHF), and vice versa. This leads to warming of the atmosphere, increasing T2m and the evaporative demand (despite the dry conditions), which further contributes to SM depletion. In other words, a positive feedback exists between temperature increase (i.e. SHF increase or EF decrease) and SM depletion. In turn, PBLH tends to increase as SHF and T2m increase, while variations in Q2m impact directly LWR. Overall, in CTL (Figure 4 a), 26 correlations are significant during clear-sky days, while in UNC (Figure 4 b) this number decreases to 12. Note that the moistening and growth of the boundary layer respond to the variability of the surface heat fluxes partition only in the CTL experiment, since there are no correlations between the heat fluxes and PBLH, T2m and Q2m in UNC. As expected, the coupling between SM and most variables is only relevant in CTL, and MSE relates more strongly to Q2m and T2m in UNC, likely because SHF and LHF are anticorrelated in CTL. Moreover, the percentage of clear-sky days is slightly reduced from CTL (8.6%) to UNC (7.2%).

On rainy-night days the coupling between SM and SHF, LHF and EF (Figure 4 c) is weaker than for clear-sky days (Figure 4 a) according to the magnitudes of the correlations, and, furthermore, there are fewer differences between CTL and UNC (23 vs 15 significant correlations, Figure 4 c,d). The local coupling changes (CTL vs UNC) for rainy-afternoon days are similar to those for rainy-night days (not shown), however, as stated previously, rainy-afternoon events do not show significant differences in precipitation amount between simulations. Consequently, the fact that precipitation in UNC is higher than in CTL for rainy nights cannot be attributed to a local coupling effect, but rather Figures 2 and 4 suggest that non-local drivers are more important (e.g. moisture transport through the SALLJ).

Discussion and conclusions

We found that rainy afternoons during the warm season in the SALLJ exit region are driven by local evapotranspiration that supplies moisture to the atmosphere, increasing the precipitable water content and triggering a precipitation event. On the other hand, nocturnal precipitation events are a consequence of moisture flux convergence in the area from external sources and are considerably stronger than afternoon events. While our results may be sensible to the choice of the precipitation thresholds and hourly ranges used for defining the events, and may also differ if another model had been used, they are nevertheless consistent with previous studies for northern Argentina (e.g. Nicolini and Saulo, 2006) and for the North American Southern Great Plains (e.g Tao et al., 2019).

Based on overall means, the precipitation intensity (frequency) is higher in the satellite products (RCA4) in northern Argentina (Giles et al., 2019). Here, we went deeper in the characterization

of afternoon and nighttime rainfall events including the recent ERA5 reanalysis. RCA4 and ERA5 agree on rain intensity, both at afternoon and night events. However, RCA4's precipitation is triggered a few hours earlier than ERA5's, a bias usually detected in climate models (Dai, 2006; Covey et al., 2016). Also, the accumulation of precipitable water before the event is considerably lower in RCA4 than in ERA5, which is tied to the early convection removing water from the atmosphere prematurely. The intensity of both types of precipitation events is markedly underestimated in both RCA4 and ERA5 compared to the satellite products and both also tend to slightly overestimate the number of rainy afternoons. However, it is on rainy nights when there is a notorious disparity between datasets, with RCA4 (ERA5) considerably underestimating (overestimating) the number of events against TRMM-3B42 and CMORPH.

Our results showed a stronger coupling between surface and near-surface variables during clear-sky days than during rainy days, which we attribute to the fact that the feedbacks during rainy days are more complex and include processes not related to the local effect of the land state. Precipitation events are influenced by different factors other than the local influence of soil moisture-atmosphere coupling (e.g. heat and moisture transport from other regions, stability and small-scale processes in the overlying atmosphere and large or regional-scale dynamic patterns). In turn, the occurrence of precipitation introduces greater temporal and spatial variability in soil moisture, and alters the water and energy balances of the surface.

In the RCA4 experiment, the UNC simulation is highly idealized because soil moisture is prescribed and does not respond to either precipitation nor evapotranspiration. Over certain regions, the uncoupled surface provides enhanced evapotranspiration without soil moisture

depletion (since soil moisture is overridden at each time step) leading to the net creation and input of water to the atmosphere. Since the atmosphere cannot store unlimited water, precipitation also increases downstream from the spurious source of evapotranspiration (Berg et al., 2014; Wei and Dirmeyer, 2019). The evaporative fraction is higher in UNC than in CTL in much of southeastern and eastern South America, including Paraguay, southern Bolivia, and eastern Brazil (see Figure 4e in Menéndez et al., 2019, who analyzed temperature variability using the same set of RCA4 experiments), indicating that the percentage of available energy that is destined for evaporation increases in UNC. This suggests that the evapotranspiration is higher in UNC than in CTL in regions upstream of JEXIT, which is consistent with the increased atmospheric moisture transport and precipitation in UNC.

We hypothesize that changes in the continental-scale circulation associated with the suppression of the interannual variability of soil moisture in UNC are responsible for the increase in moisture convergence and precipitation in the SALLJ exit region. On the other hand, less clear-sky and rainy-night days were found in the UNC simulation, indicating that local land-atmosphere coupling may affect cloudiness, and particularly, that coupling in CTL during the afternoon may favor the occurrence of precipitation in the subsequent night in spite of having less precipitable water than UNC. The specific mechanisms responsible for producing less but more intense precipitation events in UNC are still being explored and will hopefully be published in an upcoming work to improve the knowledge of soil moisture-precipitation processes in the region.

Acknowledgements

We appreciate the valuable comments of two anonymous reviewers that helped improve this manuscript. We thank the ECMWF, the Climate Prediction Center and JAXA and NASA for providing access to the ERA5, CMORPH and TRMM-3B42 datasets, respectively. The research was supported by projects LEFE (CNRS, France, AO2015-876370), PIP (CONICET, Argentina, 112-201101-00932) and PICT (ANPCyT, Argentina, 2015-3097).

References

Berbery, E. H. and Barros, V. R. (2002). The Hydrologic Cycle of the La Plata Basin in South America. Journal of Hydrometeorology, 3(6), 630–645. https://doi.org/10.1175/1525-7541(2002)003<0630:thcotl>2.0.co;2

Berbery, E. H. and Collini, E. A. (2000). Springtime Precipitation and Water Vapor Flux over Southeastern South America. Monthly Weather Review, 128(5), 1328–1346. https://doi.org/2.0.co;2">10.1175/1520-0493(2000)128<1328:spawvf>2.0.co;2

Berg, A., Lintner, B. R., Findell, K. L., Malyshev, S., Loikith, P. C. and Gentine, P. (2014). Impact of Soil Moisture–Atmosphere Interactions on Surface Temperature Distribution. Journal of Climate, 27(21), 7976–7993. https://doi.org/10.1175/jcli-d-13-00591.1

C3S, Copernicus Climate Change Service. (2017). ERA5: Fifth Generation of ECMWF Atmospheric Reanalyses of the Global Climate. https://cds.climate.copernicus.eu/cdsapp#!/home

Carril, A. F., Menéndez, C. G., Remedio, A. R. C., Robledo, F., Sörensson, A., Tencer, B., -P. Boulanger, J., de Castro, M., Jacob, D., Le Treut, H., Li, L. Z. X., Penalba, O., Pfeifer, S., Rusticucci, M., Salio, P., Samuelsson, P., Sanchez, E. and Zaninelli, P. (2012). Performance of a multi-RCM ensemble for South Eastern South America. Climate Dynamics, 39(12), 2747–2768. https://doi.org/10.1007/s00382-012-1573-z

Climate Prediction Center/National Centers for Environmental Prediction/National Weather Service/NOAA/U.S. Department of Commerce. (2018). updated daily. NOAA CPC Morphing Method (CMORPH) Global Precipitation Analyses, Version 1.0 (0.25 degree, 3-hourly resolution). Research Data Archive at the National Center for Atmospheric Research, Computational and Information Systems Laboratory.

Covey, C., Gleckler, P. J., Doutriaux, C., Williams, D. N., Dai, A., Fasullo, J., Trenberth, K. and Berg, A. (2016). Metrics for the Diurnal Cycle of Precipitation: Toward Routine Benchmarks for Climate Models. Journal of Climate, 29(12), 4461–4471. https://doi.org/10.1175/jcli-d-15-0664.1

Dai, A. (2006). Precipitation Characteristics in Eighteen Coupled Climate Models. Journal of Climate, 19(18), 4605–4630. https://doi.org/10.1175/jcli3884.1

da Rocha, R. P., Morales, C. A., Cuadra, S. V. and Ambrizzi, T. (2009). Precipitation diurnal cycle and summer climatology assessment over South America: An evaluation of Regional Climate Model version 3 simulations. Journal of Geophysical Research, 114(D10). https://doi.org/10.1029/2008jd010212

Eltahir, E. A. B. (1998). A Soil Moisture-Rainfall Feedback Mechanism: 1. Theory and observations. Water Resources Research, 34(4), 765–776. https://doi.org/10.1029/97wr03499

Falco, M., Carril, A. F., Menéndez, C. G., Zaninelli, P. G. and Li, L. Z. X. (2019). Assessment of CORDEX simulations over South America: added value on seasonal climatology and resolution considerations. Climate Dynamics, 52 (7-8), 4771–4786. https://doi.org/10.1007/s00382-018-4412-z

Ford, T. W., Rapp, A. D. and Quiring, S. M. (2015). Does Afternoon Precipitation Occur Preferentially over Dry or Wet Soils in Oklahoma? Journal of Hydrometeorology, 16(2), 874–888. https://doi.org/10.1175/jhm-d-14-0005.1

Froidevaux, P., Schlemmer, L., Schmidli, J., Langhans, W. and Schär, C. (2014). Influence of the Background Wind on the Local Soil Moisture–Precipitation Feedback. Journal of the Atmospheric Sciences, 71(2), 782–799. https://doi.org/10.1175/jas-d-13-0180.1

Giles, J. A., Ruscica, R. C. and Menéndez, C. G. (2019). The diurnal cycle of precipitation over South America represented by five gridded datasets. International Journal of Climatology, 40(2), 668-686. https://doi.org/10.1002/joc.6229

Guillod, B. P., Orlowsky, B., Miralles, D., Teuling, A. J., Blanken, P. D., Buchmann, N., Ciais, P., Ek, M., Findell, K. L., Gentine, P., Lintner, B. R., Scott, R. L., Van den Hurk, B. and Seneviratne, S. I. (2014). Land-surface controls on afternoon precipitation diagnosed from observational data: uncertainties and confounding factors. Atmospheric Chemistry and Physics, 14(16), 8343–8367. https://doi.org/10.5194/acp-14-8343-2014

Hersbach, H., Bell, B., Berrisford, P., Horányi, A., Muñoz Sabater, J., Nicolas, J., Radu, R., Schepers, D., Simmons, A., Soci, C. and Dee, D. (2019). Global Reanalysis: Goodbye ERA-Interim, Hello ERA5. ECMWF Newsletter, 159, 17–24. https://doi.org/10.21957/vf291hehd7

Holgate, C. M., Van Dijk, A. I. J. M., Evans, J. P. and Pitman, A. J. (2019). The Importance of the One-Dimensional Assumption in Soil Moisture - Rainfall Depth Correlation at Varying Spatial Scales. Journal of Geophysical Research: Atmospheres, 124(6), 2964–2975. https://doi.org/10.1029/2018jd029762

Huffman, G. J., Adler, R. F., Bolvin, D. T. and Nelkin, E. J. (2009). The TRMM Multi-Satellite Precipitation Analysis (TMPA). Satellite Rainfall Applications for Surface Hydrology, 3–22. https://doi.org/10.1007/978-90-481-2915-7_1

Huffman, G. J., Bolvin, D. T., Nelkin, E. J., Wolff, D. B., Adler, R. F., Gu, G., Hong, Y., Bowman, K. P. and Stocker, E. F. (2007). The TRMM Multisatellite Precipitation Analysis (TMPA): Quasi-Global, Multiyear, Combined-Sensor Precipitation Estimates at Fine Scales. Journal of Hydrometeorology, 8(1), 38–55. https://doi.org/10.1175/jhm560.1

Jones, C. and Carvalho, L. M. V. (2018). The influence of the Atlantic multidecadal oscillation on the eastern Andes low-level jet and precipitation in South America. npj Climate and Atmospheric Science, 1(1). https://doi.org/10.1038/s41612-018-0050-8

Joyce, R. J., Janowiak, J. E., Arkin, P. A. and Xie, P. (2004). CMORPH: A Method that Produces Global Precipitation Estimates from Passive Microwave and Infrared Data at High Spatial and Temporal Resolution. Journal of Hydrometeorology, 5(3), 487–503. https://doi.org/2.0.co;2">10.1175/1525-7541(2004)005<0487:camtpg>2.0.co;2

Kupiainen, M., Jansson, C., Samuelsson, P., Jones, C., Willén, U., Hansson, U., Ullerstig, A., Wang, S. and Döscher, R. (2014). Rossby Centre Regional Atmospheric Model, RCA4. Rossby Center News Letter.

Marengo, J. A., Soares, W. R., Saulo, C. and Nicolini, M. (2004). Climatology of the Low-Level Jet East of the Andes as Derived from the NCEP–NCAR Reanalyses: Characteristics and Temporal Variability. Journal of Climate, 17(12), 2261–2280. https://doi.org/2.0.co;2">10.1175/1520-0442(2004)017<2261:cotlje>2.0.co;2

Martinez, J. A. and Dominguez, F. (2014). Sources of Atmospheric Moisture for the La Plata River Basin. Journal of Climate, 27(17), 6737–6753. https://doi.org/10.1175/jcli-d-14-0022.1

Menéndez, C. G., Giles, J., Ruscica, R., Zaninelli, P., Coronato, T., Falco, M., Sörensson, A., Fita, L., Carril, A. and Li, L. (2019). Temperature variability and soil–atmosphere interaction in South America simulated by two regional climate models. Climate Dynamics, 53, Issues 5-6), 2919–2930. https://doi.org/10.1007/s00382-019-04668-6

Menéndez, C., Zaninelli, P., Carril, A. and Sánchez, E. (2016). Hydrological cycle, temperature and land surface-atmosphere interaction in La Plata Basin during summer: response to climate change. Climate Research 68(2), 231-241. https://doi.org/10.3354/cr01373

Montini, T. L., Jones, C. and Carvalho, L. M. V. (2019). The South American Low-Level Jet: A New Climatology, Variability, and Changes. Journal of Geophysical Research: Atmospheres, 124(3), 1200–1218. https://doi.org/10.1029/2018jd029634

Nicolini, M. and Saulo, A. C. (2006). Modeled Chaco low-level jets and related precipitation patterns during the 1997–1998 warm season. Meteorology and Atmospheric Physics, 94(1-4), 129–143. https://doi.org/10.1007/s00703-006-0186-7

Petrova, I., Miralles, D., van Heerwaarden, C. and Wouters, H. (2018). Relation between Convective Rainfall Properties and Antecedent Soil Moisture Heterogeneity Conditions in North Africa. Remote Sensing, 10(6), 969. https://doi.org/10.3390/rs10060969

Rasmusson, E. M. (1968). ATMOSPHERIC WATER VAPOR TRANSPORT AND THE WATER BALANCE OF NORTH AMERICA: II. LARGE-SCALE WATER BALANCE INVESTIGATIONS. Monthly Weather Review, 96(10), 720–734. https://doi.org/10.1175/1520-0493(1968)096<0720:awvtat>2.0.co;2

Reboita, M. S., Dutra, L. M. M. and Dias, C. G. (2016). Diurnal cycle of precipitation simulated by RegCM4 over South America: present and future scenarios. Climate Research, 70(1), 39–55. https://doi.org/10.3354/cr01416

Ruscica, R. C., Menéndez, C. G. and Sörensson, A. A. (2016). Land surface-atmosphere interaction in future South American climate using a multi-model ensemble. Atmospheric Science Letters, 17(2), 141–147. https://doi.org/10.1002/asl.635

Ruscica, R. C., Sörensson, A. A. and Menéndez, C. G. (2014). Hydrological links in Southeastern South America: soil moisture memory and coupling within a hot spot. International Journal of Climatology, 34(14), 3641–3653. https://doi.org/10.1002/joc.3930

Ruscica, R. C., Sörensson, A. A. and Menéndez, C. G. (2015). Pathways between soil moisture and precipitation in southeastern South America. Atmospheric Science Letters, 16(3), 267–272. https://doi.org/10.1002/asl2.552

Saulo, A. C., Nicolini, M. and Chou, S. C. (2000). Model characterization of the South American low-level flow during the 1997-1998 spring-summer season. Climate Dynamics, 16(10-11), 867–881. https://doi.org/10.1007/s003820000085

Solman, S. A., Sanchez, E., Samuelsson, P., da Rocha, R. P., Li, L., Marengo, J., Pessacg, N. L., Remedio, A. R. C., Chou, S. C., Berbery, H., Le Treut. H., de Castro, M. and Jacob, D. (2013) Evaluation of an ensemble of regional climate model simulations over South America driven by the ERA-Interim reanalysis: model performance and uncertainties. Clim Dyn 41, 1139–1157. https://doi.org/10.1007/s00382-013-1667-2

Song, H.-J., Ferguson, C. R. and Roundy, J. K. (2016). Land–Atmosphere Coupling at the Southern Great Plains Atmospheric Radiation Measurement (ARM) Field Site and Its Role in Anomalous Afternoon Peak Precipitation. Journal of Hydrometeorology, 17(2), 541–556. https://doi.org/10.1175/jhm-d-15-0045.1

Sörensson, A. A., and Menéndez, C. G. (2011). Summer soil—precipitation coupling in South America. Tellus A: Dynamic Meteorology and Oceanography, 63(1), 56-68.

Spennemann, P. C., Salvia, M., Ruscica, R. C., Sörensson, A. A., Grings, F. and Karszenbaum, H. (2018). Land-atmosphere interaction patterns in southeastern South America using satellite products and climate models. International Journal of Applied Earth Observation and Geoinformation, 64, 96–103. https://doi.org/10.1016/j.jag.2017.08.016

Tao, C., Zhang, Y., Tang, S., Tang, Q., Ma, H., Xie, S. and Zhang, M. (2019). Regional Moisture Budget and Land-Atmosphere Coupling Over the U.S. Southern Great Plains Inferred From the

ARM Long-Term Observations. Journal of Geophysical Research: Atmospheres, 124(17-18), 10091–10108. https://doi.org/10.1029/2019jd030585

Tawfik, A. B., Dirmeyer, P. A. and Santanello, J. A. (2015). The Heated Condensation Framework. Part II: Climatological Behavior of Convective Initiation and Land–Atmosphere Coupling over the Conterminous United States. Journal of Hydrometeorology, 16(5), 1946–1961. https://doi.org/10.1175/jhm-d-14-0118.1

Taylor, C. M., Birch, C. E., Parker, D. J., Dixon, N., Guichard, F., Nikulin, G. and Lister, G. M. S. (2013). Modeling soil moisture-precipitation feedback in the Sahel: Importance of spatial scale versus convective parameterization. Geophysical Research Letters, 40(23), 6213–6218. https://doi.org/10.1002/2013gl058511

Taylor, C. M., de Jeu, R. A. M., Guichard, F., Harris, P. P. and Dorigo, W. A. (2012). Afternoon rain more likely over drier soils. Nature, 489(7416), 423–426. doi:10.1038/nature11377

Taylor, C. M., Gounou, A., Guichard, F., Harris, P. P., Ellis, R. J., Couvreux, F. and De Kauwe, M. (2011). Frequency of Sahelian storm initiation enhanced over mesoscale soil-moisture patterns. Nature Geoscience, 4(7), 430–433. https://doi.org/10.1038/ngeo1173

Teitelbaum, H., Le Treut, H., Moustaoui, M., Cabrera, G. C. and Ibañez, G. (2008). Deep Convection East of the Andes Cordillera: A Test Case Analysis of Airmass Origin. Monthly Weather Review, 136(6), 2201–2209. https://doi.org/10.1175/2007mwr2088.1

Tropical Rainfall Measuring Mission (2011). TRMM (TMPA) Rainfall Estimate L3 3 hour 0.25 degree x 0.25 degree V7, Greenbelt, MD, Goddard Earth Sciences Data and Information Services Center (GES DISC).

van der Ent, R. J., Savenije, H. H. G., Schaefli, B. and Steele-Dunne, S. C. (2010). Origin and fate of atmospheric moisture over continents. Water Resources Research, 46(9). https://doi.org/10.1029/2010wr009127

Vera, C., Baez, J., Douglas, M., Emmanuel, C. B., Marengo, J., Meitin, J., Nicolini, M., Nogues-Paegle, J., Paegle, J., Penalba, O., Salio, P., Saulo, C., Silva Dias, M. A., Silva Dias, P. and Zipser, E. (2006). The South American Low-Level Jet Experiment. Bulletin of the American Meteorological Society, 87(1), 63–78. https://doi.org/10.1175/bams-87-1-63

Wei, J. and Dirmeyer, P. A. (2019). Sensitivity of land precipitation to surface evapotranspiration: a nonlocal perspective based on water vapor transport. Geophysical Research Letters, 46(21), 12588–12597. https://doi.org/10.1029/2019gl085613

Welty, J. and Zeng, X. (2018). Does Soil Moisture Affect Warm Season Precipitation Over the Southern Great Plains? Geophysical Research Letters, 45(15), 7866–7873. https://doi.org/10.1029/2018gl078598

Xie, P., Joyce, R., Wu, S., Yoo, S.-H., Yarosh, Y., Sun, F. and Lin, R. (2017). Reprocessed, Bias-Corrected CMORPH Global High-Resolution Precipitation Estimates from 1998. Journal of Hydrometeorology, 18(6), 1617–1641. https://doi.org/10.1175/jhm-d-16-0168.1

Zaninelli, P. G., Menéndez, C. G., Falco, M., López-Franca, N. and Carril, A. F. (2019). Future hydroclimatological changes in South America based on an ensemble of regional climate models. Climate Dynamics, 52(1-2), 819–830. https://doi.org/10.1007/s00382-018-4225-0

Zemp, D. C., -F. Schleussner, C., Barbosa, H. M. J., van der Ent, R. J., Donges, J. F., Heinke, J., Sampaio, G. and Rammig, A. (2014). On the importance of cascading moisture recycling in South America. Atmospheric Chemistry and Physics, 14(23), 13337–13359. https://doi.org/10.5194/acp-14-13337-2014

Zhang, Y. and Klein, S. A. (2010). Mechanisms Affecting the Transition from Shallow to Deep Convection over Land: Inferences from Observations of the Diurnal Cycle Collected at the ARM Southern Great Plains Site. Journal of the Atmospheric Sciences, 67(9), 2943–2959. https://doi.org/10.1175/2010jas3366.1

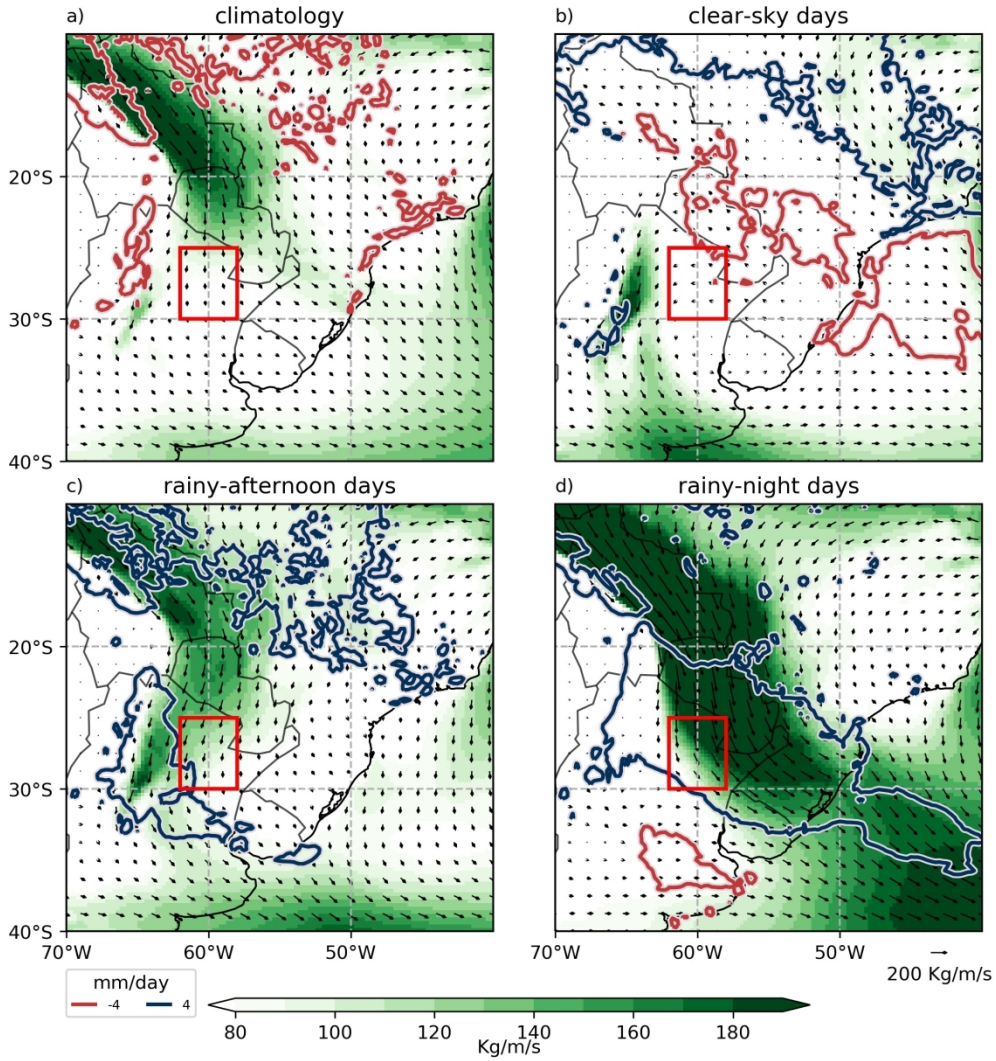

Figure 1. Spatial patterns of ERA5 vertically integrated moisture flux (vectors) in the semester October-March for the 1998-2012 period. (a) Mean climatology. Composite fields for the three types of events analyzed: (b) clear-sky days; (c) rainy-afternoon days; (d) rainy-night days. Color shading shows intensity (module of the vector). The contours outline the main areas of moisture flux convergence (blue) and divergence (red). The red rectangle indicates the JEXIT region.

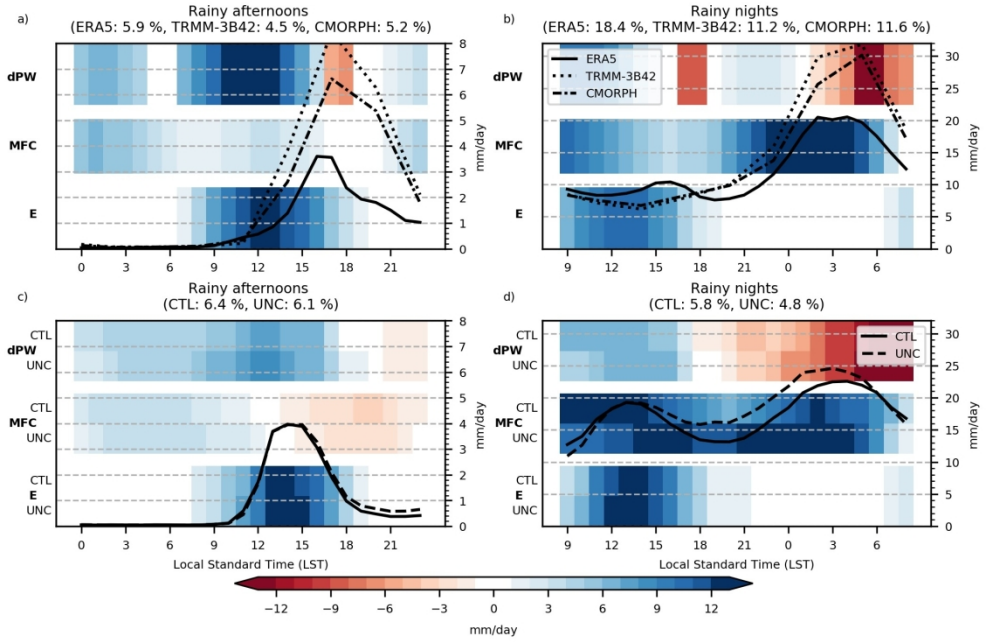

Figure 2. Diurnal cycle composites of area-averaged precipitation (P, in black lines) and evapotranspiration, vertically integrated moisture flux convergence and rate of change of atmospheric precipitable water (E, MFC and dPW respectively, in colors) for rainy-afternoon days (a,c) and rainy-night days (b,d), for ERA5 (a,b) and RCA4 CTL and UNC (c,d), in mm/day. The composites of P for TRMM-3B42 and CMORPH are also shown (a,b). The percentage of days that meet the corresponding condition is shown in between parenthesis.

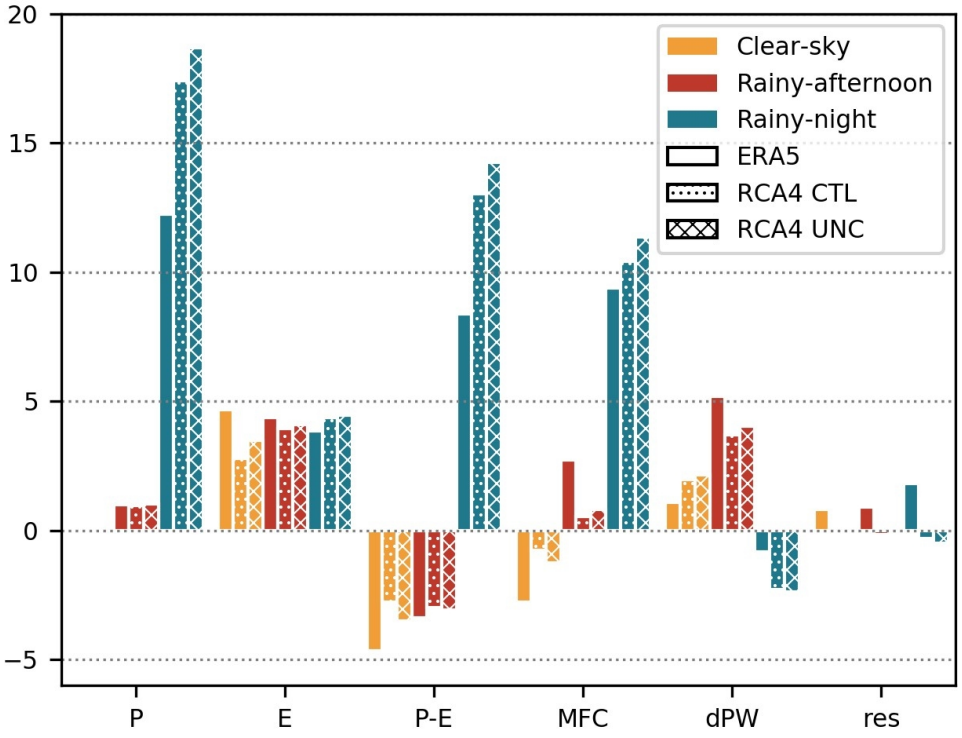

Figure 3. Mean values of daily area-averaged precipitation (P), evapotranspiration (E), P-E, vertically integrated moisture flux convergence (MFC = - MFD) and rate of change of atmospheric precipitable water (dPW) for clear-sky, rainy-afternoon and rainy-night days, for ERA5 and RCA4, in mm/day. We also show the residual from Equation (1), res = P - E + MFD + dPW.

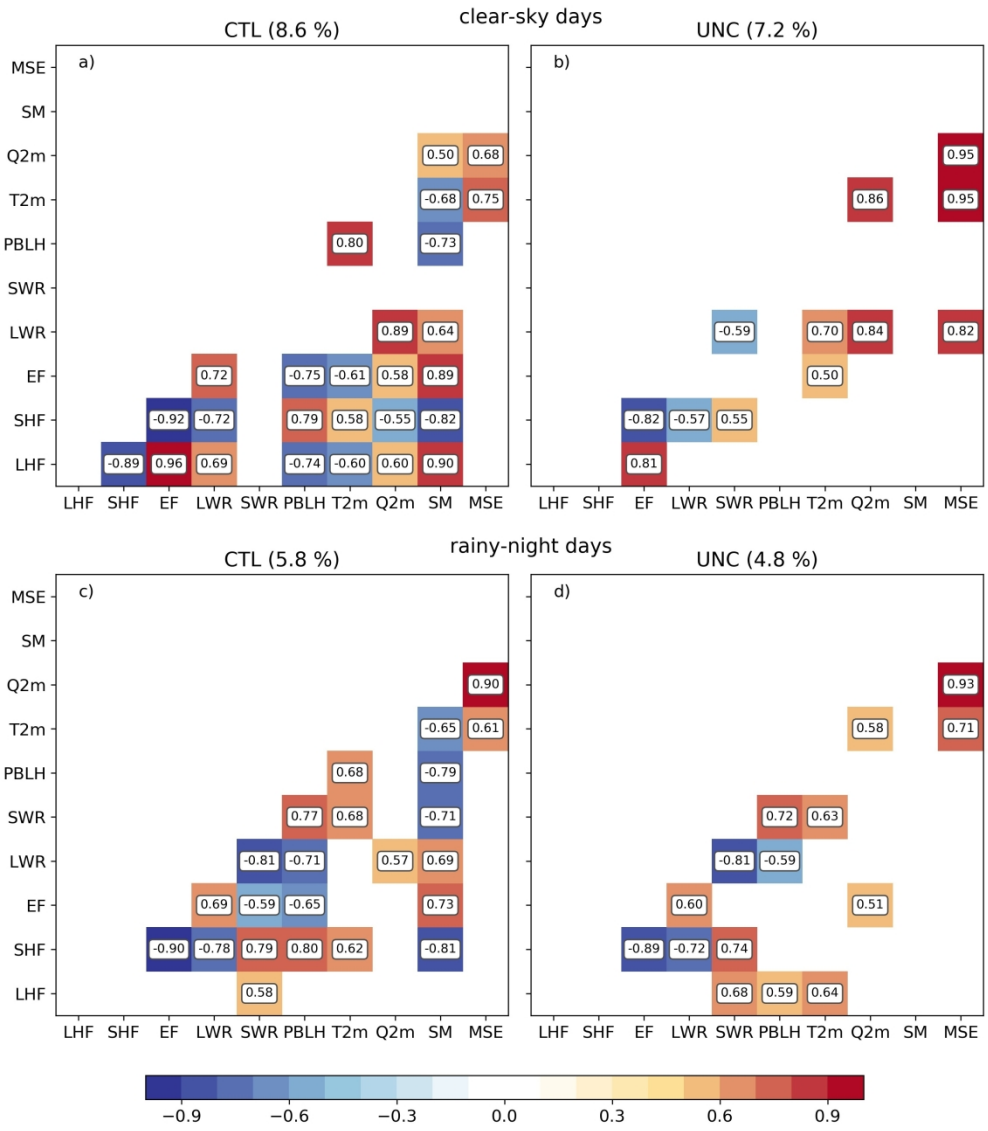

Figure 4. RCA4 correlations of daily anomalies in clear-sky (a,b) and rainy-night (c,d) days between area-averaged latent heat flux (LHF), sensible heat flux (SHF), evaporative fraction (EF), net longwave radiation (LWR), net shortwave radiation (SWR), planetary boundary layer height (PBLH), 2-meter temperature (T2m), 2-meter specific humidity (Q2m), soil moisture (SM) and moist static energy at the 900 hPa level (MSE) for each RCA4 simulation, with the percentage of days that meet the classification conditions in between parenthesis. Correlations with absolute values below 0.5 or not statistically significant at the 95% confidence level (two-tailed Student's test) are not shown.